This paper appears in Journal of Medical Robotics Research.
https://doi.org/10.1142/S2424905X20410020

Journal of Medical Robotics Research, Vol. 0, No. 0 (2020) 1–16

An Admittance-Controlled Force-Scaling Dexterous Assistive Robotic System

Jakub Piwowarczyk[a], Jay Carriere[a], Kim Adams[b], Mahdi Tavakoli[a]

[a] *Department of Electrical and Computer Engineering, University of Alberta, 116 St & 85 Ave, Edmonton, Alberta T6G 1H9, Canada*
E-mail: piwowarc@ualberta.ca (Corresponding Author); jtcarrie@ualberta.ca; mahdi.tavakoli@ualberta.ca

[b] *Faculty of Rehabilitation Medicine, University of Alberta, 116 St & 85 Ave, Edmonton, Alberta T6G 1H9, Canada*
E-mail: kim.adams@ualberta.ca

Play has a vital role in a child's development; it can affect everything from social and language to cognitive and perceptual skills. However, if a child has a physical disability, the fundamental limitations of their disability may prevent them from participating in all forms of play. Construction and block play is an example of play that may be difficult for children who have reduced upper body strength and are, therefore, unable to manipulate heavier objects in space. In this paper, we propose a novel 6 degree-of-freedom admittance-controlled, force-scaling robot that will allow for children to lift heavier objects than they would normally be able to, while still retaining the full range of motion of their upper-body. This assistive system is designed to retain the user's haptic perception, allowing the user to still partially feel the weight of the objects that they are manipulating. Two user studies are done to evaluate the usability of the system. First, to ensure that the force scaling of the system does not negatively affect a user's haptic perception, ten able-bodied individuals were asked to order a series of buckets with identical appearances but different masses from lightest to heaviest with three different force scaling factors. It was shown that the force amplification ability of the system does not significantly detract from users' ability to discriminate masses. Second, to evaluate the precision and the usefulness of the force scaling of the system, users were asked to perform a challenging peg-in-hole insertion task. Results indicate that the system has a positive effect on the ability of a user to perform the task when the assistance is necessary. However, increasing amounts of assistance, past those required for participants to complete the task without issues, do not have any significant effect. The effect of a modular reacher bar that can augment the workspace of users is investigated through a similar peg-in-hole insertion task. For the trials with the modular reacher bar attached, it is shown that the system's force amplification has a very positive effect in assisting users in completing the task. It should be noted that although the target population for this paper is children with disabilities, there can also be uses for this system as a general assistive technology for adults with upper-body weakness in their daily lives.

Keywords: Powered Assistive Technologies; Haptics; Human-Machine Interaction.

1. Introduction

The role that play has in a child's development is so significant that the United Nations High Commission has recognized it as a birthright of every child.[1] It can affect social, cognitive, perceptual, physical, emotional, and language development.[2–4] Children who have physical disabilities, however, may have reduced access to play due to the functional limitations of their impairments, which may, therefore, have a significant negative effect on their overall development.

Several assistive robotic technologies have been developed in order to bridge this gap.[4–9] Many of these technologies, however, were developed for and tested with populations with relatively significant disability. Due to this, previously developed assistive technologies tend to be limited to devices with a reduced workspace (e.g. joystick control) or two degrees of freedom (DoFs). These limitations may not be best for someone who may have a good range of motion (RoM) but not enough strength to manipulate toys in free space. It is important for children to be able to manipulate objects because of the benefits to development; for example, it has been shown that doing 3D tasks such as construction play and playing with blocks can have positive impacts on mathematical word problem-solving skills[10] and higher language scores.[11]

In this paper, a 6-DoF admittance-controlled force-scaling assistive robotic system is proposed. This system will allow a child with full RoM but reduced muscle strength to pick up and manipulate toys in free space that they would otherwise be unable to play with. In this system, an admittance model is used to allow for direct hands-on physical manipulation of the robot. Admittance controllers, similar to impedance controllers, are able to relate force and motion,[12] unlike pure position or force controllers that are only able to control a robot's position or force, respectively. For this reason, admittance-based and impedance-based controllers are widely used for physical human-robot interaction.[13] By utilizing an admittance controller, the user can directly control the motion of the robotic system through an applied force.

Through the use of two force-torque sensors, the admittance controller used in this paper was designed to take into account both the user's applied force as well as the reaction force of the environment when calculating the motion of the robot. An assistance factor is applied such that the user's input forces and torques are amplified in relation to the environmental forces and torques. This gives a user with limited muscle strength the ability to lift heavy objects while still giving them haptic perception of the environment (albeit scaled), which is also crucial to a child's development.[9,14]

To expand the use cases for this system, a modular reacher bar has also been implemented. This reacher bar allows for an extension in workspace for individuals who have a limited workspace, and would also allow for individuals who have a full RoM to reach further. This may prove especially useful for 3D play for children with reduced RoM or those who are bound to a wheelchair and have reduced strength. It can also prove useful as an assistive tool for individuals in the completion of activities of daily living.

There are several user groups that could benefit from this system. For example, individuals who have Duchenne muscular dystrophy typically develop significantly decreased muscle strength, which limits their ROM.[15] Duchenne muscular dystrophy affects roughly 1 in 3500 to 6000 male births worldwide, has an early onset, and progresses throughout life.[16] Another user group that could utilize this system is individuals who have cerebral palsy. Cerebral palsy is a permanent and non-progressive movement disorder that affects roughly 2.11 out of 1000 live births[17] and can significantly affect an individual's abilities for manual object manipulation.[8] Though these individuals may have significantly reduced ROM,[18] the reacher bar should provide them with the ability to better perform both activities of play for younger individuals and daily living for adults.

The paper is laid out as follows: Section 2 will provide an overview of related assistive robotic systems that have been developed and some background information about admittance controllers; Section 3 will outline the force-scaling admittance controller used in this study; Section 4 will describe the experimental set-up and user study; Section 5 will present and discuss the results; and Section 6 will provide concluding remarks and future plans.

2. Background

Assistive robotic technologies have been applied to assistive play for many different target use cases and populations. They may be designed for individuals of varying levels of ability. For example, for individuals who have little to no ability to generate motion, brain-computer interfaces are an excellent method to allow them to interact with an assistive system. Sakamaki et al.[19] investigated the applications of a brain-computer interface for the control of assistive robotic technologies. For individuals who may have some, but limited RoM, devices that utilize workspace scaling may be of use. Rossa et al.[20] showed that workspace scaling may be used to allow a user to control an assistive robotic system, through teleoperation, in a greater workspace volume than they can produce. Individuals may also have most to all of their RoM, but they may have other impairments such as reduced strength or lack of precision due to tremors. Jafari et al.[7,8] developed a system for individuals with cerebral palsy to be able to color within the lines utilizing haptic guidance virtual fixtures. A similar system was developed by Sakamaki et al.[6] for children with physical impairments where virtual fixtures were used to help with pick and place tasks. For an individual with a large RoM and reduced strength, one of the limitations with many of these systems is that the user's RoM cannot be fully utilized and will be restricted to the capabilities of the device that they are using. Through the use of a dexterous robotic arm, the system presented in this paper removes this limitation and allows for individuals to work within their full RoM while compensating for their reduced strength.

Many of the assistive devices described in the literature that the user physically interacts with are backdrivable, whereby they allow the user to physically move them without any control system in place to facilitate the motion. Typically, this type of control only works well for light-weight robots, as the user is forced to hold the entire weight of the robot and compensate for any dynamic forces.[21] Robots that have a larger workspace and can apply larger amounts of force, which are typically larger and heavier, are not suitable for this type of control. When the robot is not backdrivable, it necessitates the usage of a controller for the robotic system. Two models commonly used in physical human-robot interaction, for a variety of robotic systems, are impedance control and admittance control. Although impedance control systems are typically considered ideal, admittance control is usually more feasible for robots with a high mass and inertia.[22–24] Admittance control is a force-position model that has been used in many systems for physical human-robot interaction and produces specified motion of the system from force inputs.[12,22–26] Fong et al.[27] applied an admittance controller for a rehabilitational robotic system with virtual fixtures and physical human-robot interaction. Corrigan et al.[15] utilized an admittance controller to control a proof-of-concept assistive robotic arm that could be used to assist individuals with Duchenne muscular dystrophy with increasing RoM and daily tasks of living. The system in this paper expands on the previously mentioned proof-of-concept system by adding a second force-torque sensor. This second force-torque sensor will allow users to receive direct but scaled haptic feedback from the robot's interactions with the environment.

3. Robot Control

In this section, the force-scaling admittance controller used throughout this paper will be presented. To allow for the ability to scale the forces applied by the user on the robot in relation to the measured force from the environment, separate force-torque sensors are used to measure each input. To facilitate user/robot interaction, a handle is mounted on the user-side force-torque sensor. For the interaction with the environment, various end-effectors are mounted onto the tool-side force-torque sensor during this study. For example, Figure 1 shows the experimental set-up used for one of the user-studies where a hook is attached.

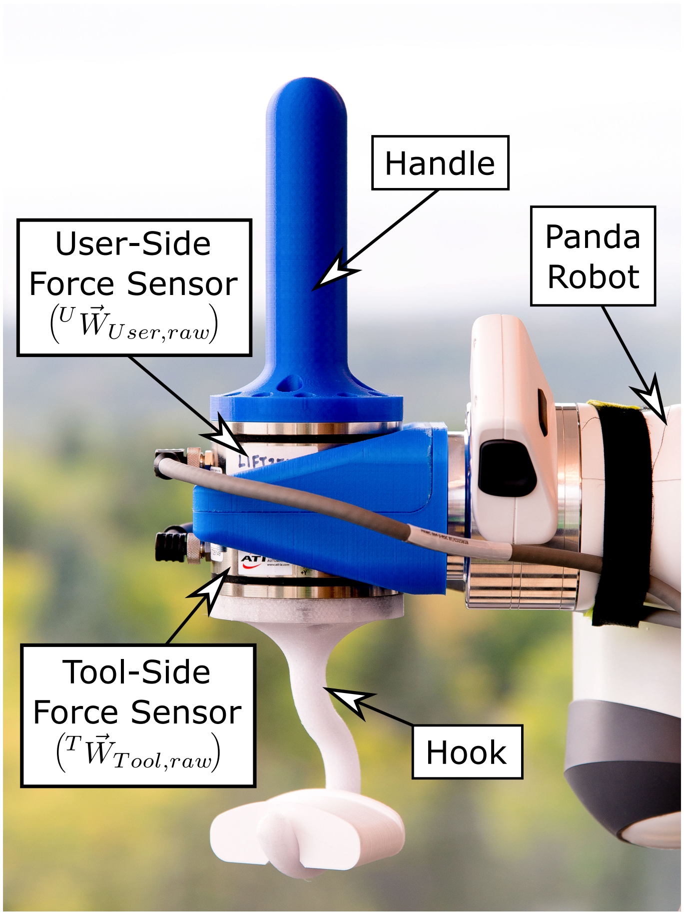

Fig. 1. Close-up of the designed handle and tool for the mass discrimination task.

In order to effectively describe the controller, some terminology must be defined. Four reference frames will be used: $\{B\}$ indicates the robot base frame, $\{U\}$ indicates the frame of the user-side force-torque sensor, $\{T\}$ indicates the frame of the tool-side force-torque sensor, and $\{S\}$ indicates a general sensor frame in the case that general formulas are presented for both sensors. Forces and torques that are read by the force-torque sensors will be denoted as wrenches where a wrench is defined as $\vec{W} = \left[\vec{F},\, \vec{\tau}\right] = [F_x,\, F_y,\, F_z,\, \tau_x,\, \tau_y,\, \tau_z]$. Angles and rotations will be defined utilizing standard $x-y-z$ Tait-Bryan angles and rotation matrices. The overall controller design that will be presented is outlined in Figure 2.

3.1. *Handle and Tool Mass Compensation*

One of the challenges in attaching various end effectors to the system is that they may produce significant forces and moments that must be compensated for, in order to maximize the usability of the system. To compensate for the weights of these attachments, the mass and center of mass of each attachment is modelled and calculated. This is done by minimizing the differences between measured and modelled gravitational wrenches by the optimization of the modelled mass parameters of each attachment. These optimized values are then used in a feed-forward model that estimates, and compensates for, the gravitational wrench generated by each attachment. This is done for all attachments on both the user-side and tool-side force-torque sensors. Due to the low intended speeds of motion of the system, the dynamics of these attachments are considered to be small and are not compensated for.

In order to perform this mass parameter calculation procedure, the robot is set to a series of eight positions and the gravitational forces and moments are measured for each. The position and orientation of robot is given as $\vec{P_i} = [x_i, y_i, z_i, \phi_i, \theta_i, \psi_i]$ and for each position, the expected gravitational wrench is calculated through the following operations: First the gravitational force in the base frame, ${}^{B}\vec{F}_{g,model}$, is calculated from the model mass, m_{model}, and gravity, $\vec{g}$, such that

$$^{B}\vec{F}_{g,model} = m_{model} \cdot \vec{g} \tag{1}$$

Next, the gravitational force is rotated to the sensor frame by the transformation

$$^{S}\vec{F}_{g,model} = ^{S}_{B}T\, ^{B}\vec{F}_{g,model} \tag{2}$$

where ${}^{S}_{B}T$ is a general transformation from a sensor frame to the robot base frame. Then, the resultant torques are calculated from the offset of the center of mass from the center of motion, $\vec{r}_{model}$ through

$$^{S}\vec{\tau}_{g,model} = \vec{r}_{model} \times {}^{T}\vec{F}_{g,model} \tag{3}$$

Finally, the total gravitational wrench calculated from the model, $\vec{W}_{g,model}$, is assembled from the gravitational force and torque in the sensor frame, giving

$$^{S}\vec{W}_{g,model} = \left[{}^{S}\vec{F}_{g,model}\ {}^{S}\vec{\tau}_{g,model}\right] \tag{4}$$

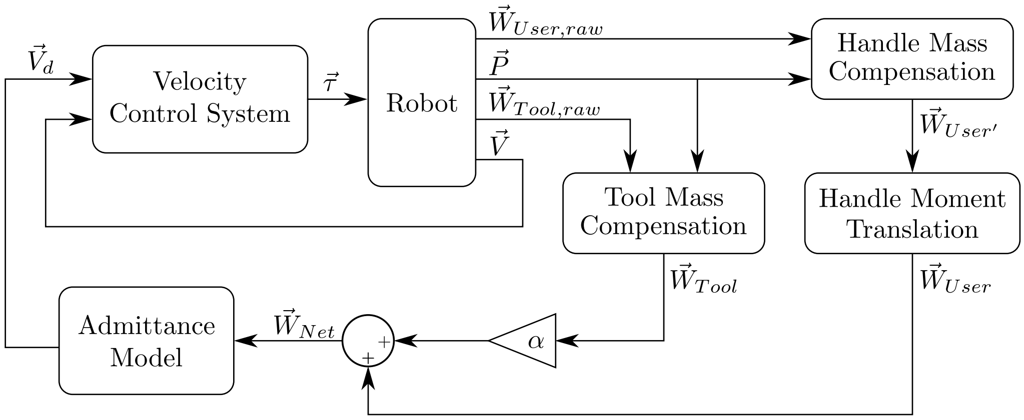

Fig. 2. Admittance controller and force scaling loop.

The values for m_{model} and $\vec{r}_{model}$ are then computed by using an equation solver to optimize

$$\min_{m,\vec{r}_{model}} \left(\sum_{i=1}^{8} |\vec{W}_{g,actual_i} - \vec{W}_{g,model_i}(m, \vec{r}_{model})| \right) \quad (5)$$

where $\vec{W}_{g,actual_i}$ is the gravitational wrench measured by the force-torque sensor at a position i and $\vec{W}_{g,model_i}$ is the gravitational wrench estimated by the model at position i. The masses and centers of masses of the attachments are optimized until the model accurately estimates the measured forces at all positions.

After all of the masses and locations of the centers of masses are calculated, the calculated model gravitational wrenches can be subtracted from the measured wrenches from the force-torque sensor to make the robot weightless and easy to control. For the user side

$$^U\vec{W}_{User'} =^U \vec{W}_{User,raw} -^U \vec{W}_{g,model,user} \quad (6)$$

where $^U\vec{W}_{User,raw}$ is the raw wrench measured by the user-side force-torque sensor, and $^U\vec{W}_{User'}$ is the user-side force-torque sensor wrench after gravity compensation. Similarly for the tool wrench,

$$^T\vec{W}_{Tool} =^T \vec{W}_{Tool,raw} -^T \vec{W}_{g,model,tool} \quad (7)$$

where $^T\vec{W}_{Tool,raw}$ is the raw wrench measured by the tool-side force-torque sensor, and $^T\vec{W}_{Tool}$ is the tool-side force-torque sensor wrench after gravity compensation.

3.2. *Handle Moment Translation*

To make the system more intuitive to use, a moment translation was applied such that moments applied by the user were measured about the center of the user input handle rather than the measuring surface of the force-torque sensor. This was achieved by calculating the effective moment of the applied forces about the center of the handle and then subtracting that result from the measured moments,

$$^U\vec{\tau}_{User} =^U \vec{\tau}_{User'} - \vec{r}_{to\,handle\,center} \times^U \vec{F}_{User'} \quad (8)$$

where $\vec{r}_{to\,handle\,center}$ is the distance from the measuring plate of the user-side force-torque sensor to the center of the user input handle and $^U\vec{\tau}_{User}$, is applied user torque about the center of the handle. This torque can then be placed into a new user wrench term as follows

$$^U\vec{W}_{User} = \left[^U\vec{F}_{User'}, {}^U\vec{\tau}_{User} \right] \quad (9)$$

where $^U\vec{W}_{User}$ is the measured wrench applied by the user about the center of the user input handle.

3.3. *Admittance Controller*

Now that the masses of the end effectors attached have been compensated for, the measurements from each force-torque sensor are transformed to the robot base frame. The user wrench is transformed by

$$^B\vec{W}_{User} = {}^B_U\mathbf{T}\,{}^U\vec{W}_{User} \quad (10)$$

where $^U\vec{W}_{User}$ represents the wrench read by the user-side sensor in its frame and ^B_UT is the transformation from the user-side sensor frame to the robot base frame. Transformation matrices are applied using two rotation matrices that act separately on the forces and torques within the wrenches. This can be shown by

$$\mathbf{T} = \begin{bmatrix} \mathbf{R} & 0 \\ 0 & \mathbf{R} \end{bmatrix} \quad (11)$$

where $\mathbf{R}$ is a standard $x-y-z$ Tait-Bryan rotation matrix. These rotation matrices are derived from the robot position and orientation, $\vec{P}$.

Likewise, the input wrench from the tool-side force-torque sensor is transformed into the robot base frame by

$$^B\vec{W}_{Tool} = {}^B_T\mathbf{T}\,{}^T\vec{W}_{Tool} \quad (12)$$

where ${}^{T}\vec{W}_{Tool}$ represents the wrench read by the tool-side force-torque sensor in its frame and ${}^{B}_{U}T$ is the transformation from the tool-side force-torque sensor frame to the robot base frame.

Next, the forces from the sensors are summed together, with the force from the tool-side of the robot being scaled

$$^{B}\vec{W}_{Net} = ^{B}\vec{W}_{User} + \alpha ^{B}\vec{W}_{Tool} \tag{13}$$

where ${}^{B}\vec{W}_{Net}$ is the net wrench on the robot in base frame after force scaling and summation and α is the scaling factor of the forces from the end effector of the robot. An assistance factor κ will be defined as

$$\kappa = \frac{1}{\alpha}$$

to represent the magnitude of the scaling of the user force relative to the tool force. This can be mathematically denoted as

$$^{B}\vec{W}_{Net} = \frac{\kappa ^{B}\vec{W}_{User} + ^{B}\vec{W}_{Tool}}{\kappa} \tag{14}$$

It should be noted that κ is only used as a reference and all scaling was done using the scaling factor, α.

The calculated net wrench is then fed into the admittance model, which is implemented according to the transfer function

$$H(s) = \frac{^{B}\vec{V}_{d}(s)}{^{B}\vec{W}_{Net}(s)} = \frac{1}{\mathbf{M}s + \mathbf{B}} \tag{15}$$

where $\vec{V}_{d}(s)$ is the resulting desired Cartesian and angular velocity in robot base frame, $\mathbf{M}$ represents the specified virtual mass and inertia matrix, and $\mathbf{B}$ represents the specified virtual Cartesian and angular damping matrix. This controller omits the stiffness parameter as restoring forces are not desirable for co-manipulation in free-space.[28] The desired velocity from the admittance controller is then streamed into a velocity control system for the robot. This eliminates the need to take into account the dynamic parameters, while still allowing for responsive force control of the system. The mass matrix was defined as

$$\mathbf{M} = \begin{bmatrix} m & 0 & 0 & 0 & 0 & 0 \\ 0 & m & 0 & 0 & 0 & 0 \\ 0 & 0 & m & 0 & 0 & 0 \\ 0 & 0 & 0 & I & 0 & 0 \\ 0 & 0 & 0 & 0 & I & 0 \\ 0 & 0 & 0 & 0 & 0 & I \end{bmatrix} \tag{16}$$

where m and I were the admittance control mass and inertia, respectively. The damping matrix was defined as

$$\mathbf{B} = \begin{bmatrix} b_c & 0 & 0 & 0 & 0 & 0 \\ 0 & b_c & 0 & 0 & 0 & 0 \\ 0 & 0 & b_c & 0 & 0 & 0 \\ 0 & 0 & 0 & b_r & 0 & 0 \\ 0 & 0 & 0 & 0 & b_r & 0 \\ 0 & 0 & 0 & 0 & 0 & b_r \end{bmatrix} \tag{17}$$

where b_c and b_r were the admittance control Cartesian and rotational dampers, respectively.

3.4. *Reacher Bar*

As previously mentioned, to augment the workspace of a user as well as allow for users with reduced RoM to make full use of the system, a modular reacher bar may be installed. An image of the system with a reacher bar used in the user trials is shown in Figure 3.

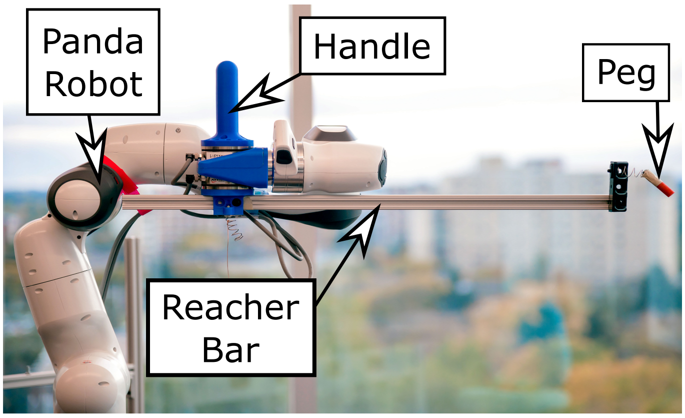

Fig. 3. Experimental equipment and set-up with reacher bar.

When the user picks up an object using the reacher bar, they must support the weight of the object they are interacting with, in addition to the torque generated by the object on the system. In the case of long reacher bars, this torque may become disproportionately large in comparison with the mass of the object itself. To account for this, the moments read from the tool-side force-torque sensor may be neglected and only the translational forces used in the admittance model. This can be achieved by modifying the scaling factor α from a scalar to a matrix of the form

$$\mathbf{A} = \begin{bmatrix} \alpha & 0 & 0 & 0 & 0 & 0 \\ 0 & \alpha & 0 & 0 & 0 & 0 \\ 0 & 0 & \alpha & 0 & 0 & 0 \\ 0 & 0 & 0 & 0 & 0 & 0 \\ 0 & 0 & 0 & 0 & 0 & 0 \\ 0 & 0 & 0 & 0 & 0 & 0 \end{bmatrix} \tag{18}$$

Although this removes three degrees of freedom of environmental feedback, it may make the control of the system easier.

In addition, for the mass compensation of the reacher bar, its mass and center of mass were estimated separately using a scale and basic principles of mass distribution rather than the estimation method defined in Section 3.1. This was done for convenience as the length of the bar would make it difficult to calibrate the system through the previously chosen 8 positions. The bar was modelled as a slender-beam and the center of mass was assumed to lie in the center of the bar. The masses of any end-effectors were also weighed and taken into account using basic mass distribution principals.

4. Experimental Setup and Protocol

In this study, two Axia80-M20 force-torque sensors (ATI Industrial Automation, Apex, NC, USA) were mounted on a Panda Robotic Arm (Franka Emika GmbH, Munich, Germany) using 3D-Printed mounting hardware. A 3D-printed handle and 3D-printed tools were used as the attachments for the force-torque sensors. This novel end-effector set-up is shown in Figure 1. The admittance controller was programmed and implemented in MATLAB 2019a (The MathWorks Inc, Natwick, MA, USA) and ran using a Simulink Simulation on a PC running Ubuntu 16.04 LTS, containing an Intel Core i5-8400 running at 4.00 GHz (Intel Corporation, Santa Clara, CA, USA). The velocity controller was coded in C++ and implemented in Robot Operating System (ROS) making use of the Franka Control Interface library for the Panda. Communication between Simulink and ROS was done over UDP and the entire control loop was run at 1 kHz. The internal control loop of the Panda also runs at 1 kHz.

In order to test the system, two separate user trials were performed. The first user trial was based on a mass discrimination task, outlined in Section 4.1, where users were asked to use the system to lift weighted buckets and order them by weight. This trial was used to verify that the system does not significantly affect a user's ability to sense their environment. The second user trial tested the positional precision that a user can achieve with the system through two peg-in-hole tasks. One task was performed without the reacher bar, and one with. For the peg-in-hole task with the reacher bar, user performance was evaluated both with and without the moment compensation described in Section 3.1. To test the usefulness of the force scaling assistance feature of the system, a virtual mass was added to the peg for both of these trials to make the task sufficiently difficult for participants to accomplish. The peg-in-hole tasks are outlined in Section 4.2.

The mass discrimination task was performed by a group of ten university students and post-doctoral fellows without disability, eight male and two female, nine right-handed and one left-handed, between the ages of 20 and 35. The peg-in-hole tasks were performed by a different group of ten university students and post-doctoral fellows (also without disability). These participants were aged between 20 and 29 years old, eight male and two female, and all of them were right-handed. This user study was approved by the University of Alberta Health Research Ethics Board Pro00057919.

For all three of the user trials, the m and I values, used in the admittance control matrices $\mathbf{M}$ and $\mathbf{B}$ covered in Sec. 3.3, were set to be $5.625\,\mathrm{kg}$ and $0.375\,\mathrm{kg}\cdot\mathrm{m}^2$ respectively and b_c and b_r, were set to be $11.25\,\frac{\mathrm{N\cdot s}}{\mathrm{m}}$ and $0.75\,\frac{\mathrm{N\cdot m\cdot s}}{\mathrm{rad}}$ respectively. These admittance control mass, inertia, and damping parameters were chosen empirically to reduce the impedance (force needed to move the system - greater mass and damping will result in a greater impedance) of the system as much as possible while still maintaining stability. The chosen virtual mass and damper values are low enough for easy movement of the system. Lower values are possible, but may require additional tuning of the control loop. However, it should be noted that these parameters can be modified as needed to best accommodate for any potential users of the system. It would be easy to implement greater impedances in certain degrees of freedom to help filter involuntary movements or tremor[a] (increased mass and damping act as a low pass filter[29]). In addition, it would also be possible to implement a tuned low-pass or notch filter to more aggressively filter certain tremor frequencies.

4.1. *Mass Discrimination Task*

For the mass discrimination task, four identical (in appearance) metal pails were filled with sand to attain masses of 1.5 kg, 2.0 kg, 2.5 kg, and 3.0 kg. The overall experimental equipment and set-up are shown in Figure 4. The participants were asked to use the system to lift the four metal pails one by one and attempt to order them from lightest to heaviest.

This task was performed at three scaling factors: $\alpha =$ 1.0, 0.5, and 0.3. These scaling factors are equivalent to assistance factors: $\kappa =$ 1.0, 2.0, and 3.0. For each trial, the order of the scaling factors used was selected from a random permutation of the three scaling factors being investigated to reduce the potential confounding effects from the users learning the task over time.

The weighing process was conducted as follows: a weighted pail would be placed in a designated spot in front of the participant, they would pick it up with the system and get a sense of the weight. After putting the pail down, it would be replaced with a different pail. The participants were allowed to weigh each pail as many times as they desired until they were confident with the order they guessed. The pails were all weighed in the same spot in an attempt to remove any confounding effects from the position dependence of the kinematics and manipulability of the Panda Arm. In addition, this removed any confounding effects from the participants picking up each bucket with a different arm orientation. The orders listed by participants were recorded and the task was repeated for the remaining scaling factors.

At the end of the session, a usability questionnaire was administered to gauge the participants' overall perception of the usability of the system. The usability questionnaire consisted of rating the following aspects of the system on a 5-point Likert Scale (1 = bad, 5 = good): manipulability (ease of using the robot to accomplish the task), confidence in using the system, sense of environment, ability to distinguish different masses during trial one, ability to distinguish

[a]This can be seen through the similarity in transfer functions between the admittance model, Eq. (15), and a first-order low-pass filter.

different masses during trial two, and ability to distinguish different masses during trial three. The mass distinguishing questions were labelled according to the trial number rather than the assistance factor due to the randomization of the order that the assistance factors were tested in. This was thought to make it easier for the participants to answer the questions.

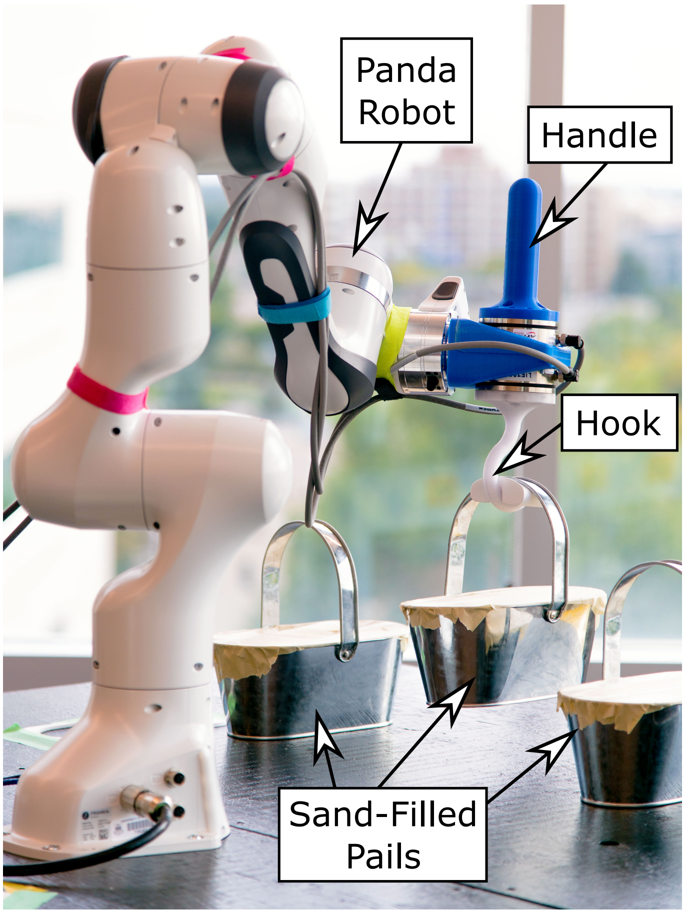

Fig. 4. Experimental equipment and set-up for the mass discrimination task.

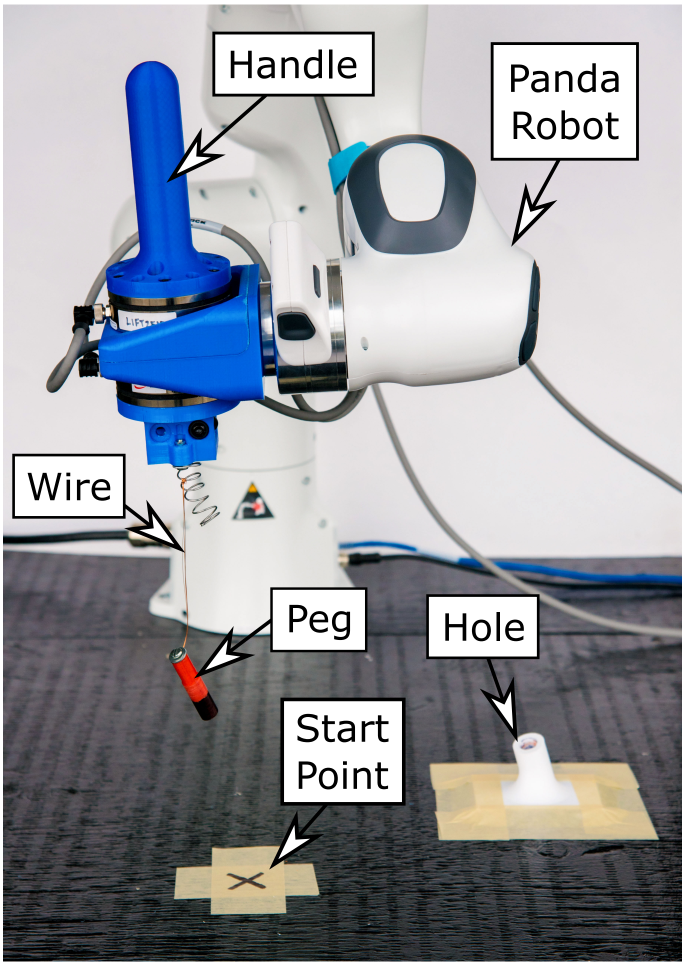

Fig. 5. Experimental equipment and set-up for the peg-in-hole task.

4.2. *User Positional Precision Tasks*

There were two tasks completed to evaluate the positional precision of a user when using the system. One, placement of a peg into a hole at an oblique angle directly under the end effector was considered (Figure 5). The second task consisted of placement of a peg into a hole at a distance with the modular reacher arm attached (Figure 6), which was evaluated with and without the moment compensation described in Section 3.4. As can be seen from the figures, the holes in the first and second tasks were mounted to horizontal and vertical walls, respectively.

As with the mass discrimination tasks, each of these tasks were performed at three scaling factors: $\alpha = 1.0$, 0.5, and 0.3, which are equivalent to assistance factors: $\kappa = 1.0$, 2.0, and 3.0. For each participant, a random order of the peg-in-hole task, the peg-in-hole task with reacher bar and no moment compensation, and the peg-in-hole task with reacher bar and moment compensation enabled was chosen. For each of these tasks, the order of assistance factors that were used was also randomized. This was done to mitigate the potential confounding effects from the participants learning the tasks.

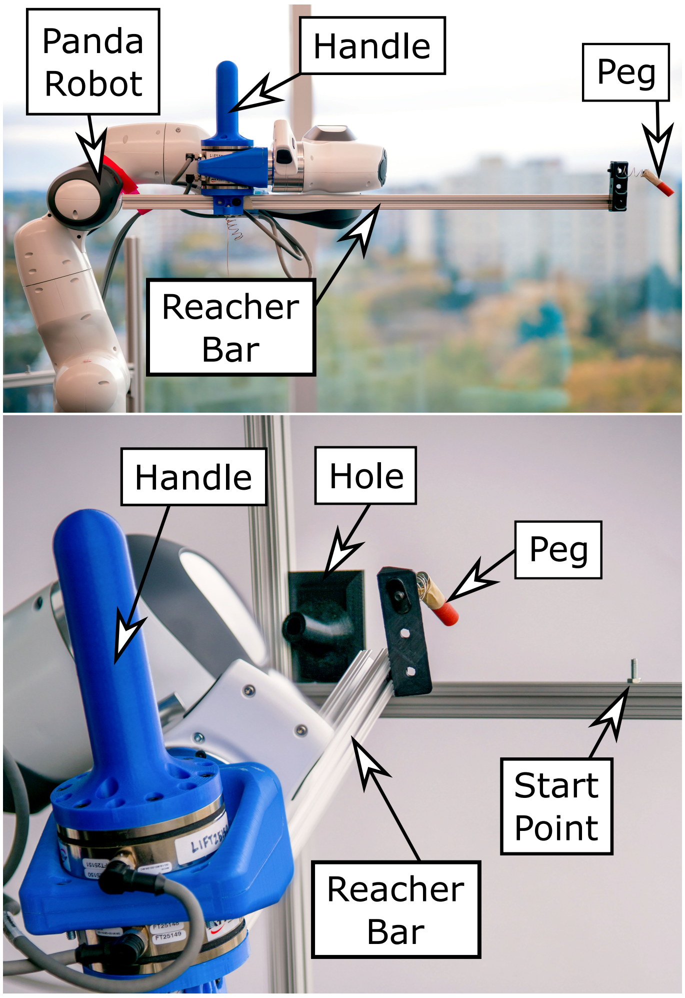

Fig. 6. Experimental equipment and set-up for the peg-in-hole tasks with reacher bar.

For both tasks, participants were asked to start at the specified starting point and then place the peg at least 75% into the hole, remove the peg, and return to the starting point. Participants were given one minute to perform as many peg insertions as they could. After the trials, a usability questionnaire was administered to gauge the participants' overall perception of the system for this task. As with the first task, the usability questionnaire consisted of rating the following aspects of the system on a 5-point Likert Scale (1 = bad, 5 = good): manipulability (ease of using the robot to accomplish the task), confidence in using the system, position accuracy, and usefulness of lifting assistance.

Peg-in-hole tasks are typically described by a precision value,[30] I, which quantifies how difficult the task is:

$$I = \log_2 \left(\frac{d_h}{d_h - d_p} \right) \tag{19}$$

where d_h is the diameter of the hole and d_p is the diameter of the peg. The measured dimensions of the peg and hole for the first setup are $d_p = 12.45$ mm and $d_h = 12.95$ mm. The precision value of this task is 4.7. For the setups with the reacher bar the dimension of the peg and hole are $d_p = 12.45$ mm and $d_h = 12.90$ mm. The precision value of this task is 4.8. Overall, these precision values are within the range of other studies that have used peg in hole tasks as a precision metric.[30,31]

Since the study was done with individuals without disability, a relatively heavy weight needed to be added to the mass of the physical peg to produce a sufficiently difficult task. The goal was to select a weight capable of emulating the difficulty of the task that an individual with a weakened upper body might experience on a day to day basis. Rather than attempting to find a very heavy peg or sufficient physical weights to do so, a virtual weight was included for each trial. A modified control loop, including the model for the weight, can be seen in Figure 7.

For the first task, a weight of 7.5 kg was modelled and for the second and third tasks, a weight of 1.25 kg was modelled at the tip of the reacher bar, which was 0.6 m away from the handle. The effect of gravity was modelled by a constant downward acceleration to create a realistic sensation of weight to the peg. This is similar to the process that was outlined for gravity compensation in Section 3.1, except instead of subtracting the calculated forces, they were added to the net tool wrench. Due to the large values of the gravitational wrenches being applied, users were always given the option of not completing, or not starting a trial, if they felt it was too heavy for them. If a user stopped a trial partway through, the number of peg insertions they completed was recorded, but it was noted that they were unable to finish the trial completely.

5. Results and Discussion

The results from the completed trials are presented and discussed in the following sections. Section 5.1 contains the results from the mass discrimination task and Section 5.2 contains the results from both the peg-in-hole task as well as the peg-in-hole task with the reacher bar.

5.1. *Mass Discrimination Task*

The results from the mass discrimination task are organized per scaling factor and the fraction correct placement of each bucket was calculated by summing the number of times the bucket was in the correct spot divided the total number of trials. The results for this task are shown in Figure 8. It should be noted that all errors that the participants made were between two neighboring buckets, i.e. misplacing the 2.5 kg and 3.0 kg buckets or the 2.0 and 2.5 kg buckets, respectively. The bucket orders recorded for each participant at each assistance level can be found in Table 1. The processed correct/incorrect data used to generate the plot can be found in Table 2.

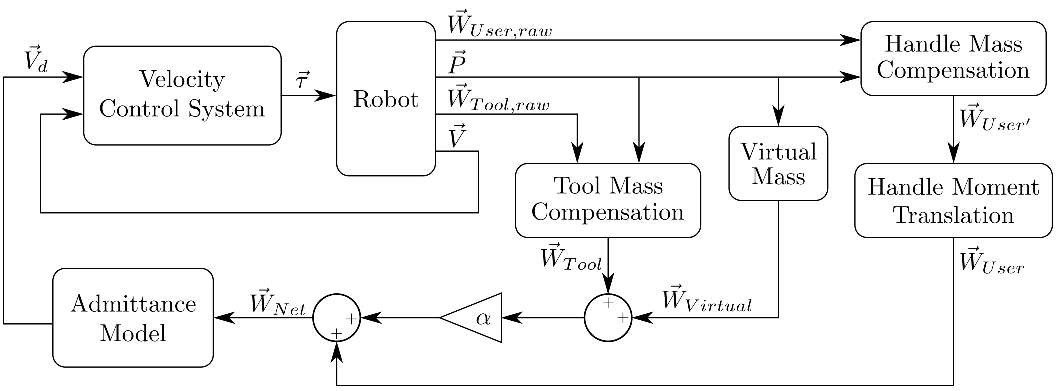

Fig. 7. Admittance controller and force scaling loop with artificial mass.

Table 1. Orders of the weighted buckets recorded at each assistance factor.

Participant Number	Assistance Factor 1.0				2.0				3.0			
1	1	3	2	4	1	2	3	4	1	2	4	3
2	1	2	3	4	1	2	3	4	1	2	3	4
3	1	2	3	4	2	1	3	4	1	2	3	4
4	1	2	3	4	1	2	3	4	1	2	3	4
5	1	2	3	4	1	2	3	4	1	2	3	4
6	1	2	3	4	1	2	3	4	2	1	3	4
7	1	2	3	4	1	2	3	4	1	2	4	3
8	1	2	3	4	1	2	3	4	1	2	3	4
9	1	2	3	4	1	2	3	4	1	2	3	4
10	1	2	3	4	1	2	4	3	1	2	3	4

Table 2. Buckets ordered correctly at each assistance factor.

Participant Number	Assistance Factor 1.0				2.0				3.0			
1	1	0	0	1	1	1	1	1	1	1	0	0
2	1	1	1	1	1	1	1	1	1	1	1	1
3	1	1	1	1	0	0	1	1	1	1	1	1
4	1	1	1	1	1	1	1	1	1	1	1	1
5	1	1	1	1	1	1	1	1	1	1	1	1
6	1	1	1	1	1	1	1	1	0	0	1	1
7	1	1	1	1	1	1	1	1	1	1	0	0
8	1	1	1	1	1	1	1	1	1	1	1	1
9	1	1	1	1	1	1	1	1	1	1	1	1
10	1	1	1	1	1	1	0	0	1	1	1	1

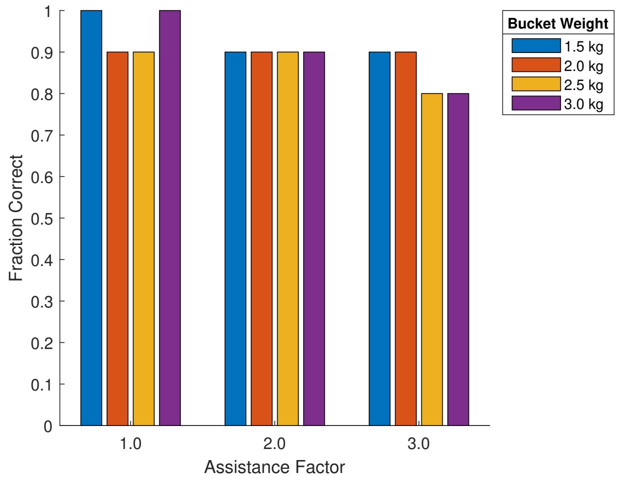

Fig. 8. Results from the mass discrimination task.

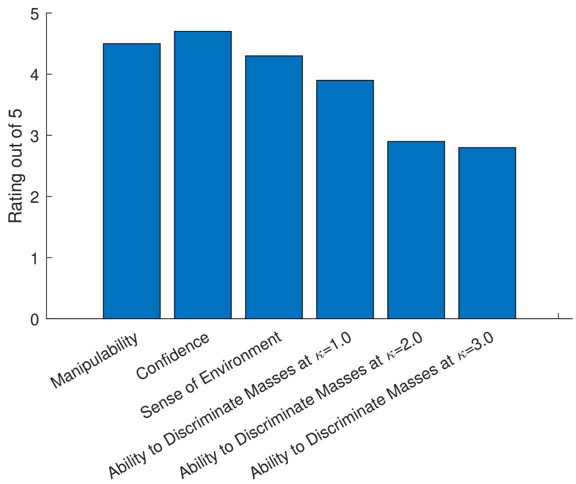

Fig. 9. Answers to the usability questionnaire for the mass discrimination task.

It can be seen that, although the overall mass discrimination of the users went down slightly as force amplification was increased, the users were still able to discriminate the masses 85% of the time. The slight lowering of mass discrimination ability is likely caused by the virtual mass and damper that is contained within the admittance controller model. This admittance control mass and damper effectively reduce the percentage difference between the dynamic masses of the pails, thereby making it harder to differentiate. It should be noted that only the dynamic forces of handling the pails are affected by the admittance control parameter. This is because the user feels no gravitational force from the robotic system or the admittance control mass; however, once they begin to move the robotic system, they begin to feel the inertial and damping characteristics of the admittance controller. It should be noted that only the forces and torques of the tool side are scaled and not those of the virtual mass and damper. For example, the percentage difference between the dynamic masses of the 2.5 kg and the 3.0 kg bucket is normally $d_{percent} = (2.5kg - 3.0kg)/(2.5kg) = 20\%$, however with the dynamic mass of the admittance model, this percent difference goes down to: $d_{percent} = ((2.5kg + 5.625kg) - (3.0kg + 5.625kg)/(2.5kg + 5.625kg) = 6.15\%$.

The results from the usability questionnaire can be found in Table 3 and the averaged data can be found in Figure 9. From the answers collected, it can be seen that, overall, the usability metrics like manipulability, confidence in the system, and sense of environment were rated quite high. In line with the experimental results, user's perception of their ability to differentiate masses goes down as the assistance of the system increases. This is to be expected though; as mentioned above, the mass of the admittance model used reduces the percent differences between the dynamic masses of the buckets. Overall though, users still rated the force scaling of the system quite well, even with the decrease in the perceived mass discrimination ability.

Overall, from the results presented from this user study, it can be seen that although the users' ability to differentiate between masses was slightly compromised with the lifting assistance enabled, their absolute ability was still retained with the users able to reach 85% accuracy even with the highest amount of assistance.

5.2. *Peg-in-Hole Task*

The results from the peg-in-hole task are plotted in Figure 10. The number of successes were normalized to each participant's maximum over each scaling factor for each participant to account for the differences in participant's talent to place pegs in holes, i.e.:

$$N_i' = \frac{N_i}{\max\left(N_{i,participant}\right)} \tag{20}$$

where N_i' is the participant normalized number of successes, N_i is the number of a successes that a participant attained in a minute at a given assistance factor, and $\max\left(N_{i,participant}\right)$ is the maximum number of successes that a participant achieved at any gain level for the peg-in-hole task.

Table 3. Tabulated answers to the usability questionnaire for the mass discrimination task.

	Number of Participants					
Rating Given for Question	0	1	2	3	4	5
Manipulability			1		2	7
Confidence				1	1	8
Sense of Environment				2	3	5
Ability to Discriminate Masses at $\kappa = 1.0$				4	3	3
Ability to Discriminate Masses at $\kappa = 2.0$		1	2	4	3	
Ability to Discriminate Masses at $\kappa = 3.0$		2	1	4	3	

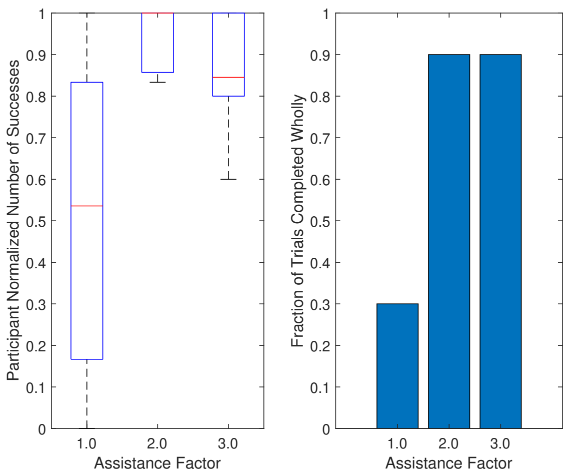

Fig. 10. Participant normalized number of successes and task completion rate at each scaling factor for the peg-in-hole task.

Table 4. Number of participant successes at each assistance factor for the peg-in-hole task.

Participant Number	Assistance Factor		
	1.0	2.0	3.0
1	0*	5	3
2	1*	2*	2*
3	5*	6	4
4	3	5	4
5	4*	6	7
6	2*	5	5
7	6	5	6
8	1*	6	5
9	7	6	6
10	0*	5	4

* indicates that the participant did not complete the trial fully.

Table 5. Participant normalized number of successes at each assistance factor for the peg-in-hole task.

Participant Number	Assistance Factor		
	1.0	2.0	3.0
1	0.00*	1.00	0.60
2	0.50*	1.00*	1.00*
3	0.83*	1.00	0.67
4	0.60	1.00	0.80
5	0.57*	0.86	1.00
6	0.40*	1.00	1.00
7	1.00	0.83	1.00
8	0.17*	1.00	0.83
9	1.00	0.86	0.86
10	0.00*	1.00	0.80

* indicates that the participant did not complete the trial fully.

The tabular data collected during these experiments can be found in Table 4 and the normalized data, which is plotted, can be found in Table 5.

The fraction of users who were able to support the weight of the peg and perform the task for the whole minute is also plotted. From these results, it can be seen that there is a significant increase in the successes from when no assistance is provided by the system ($\kappa = 1.0$), as only 30% participants completed the task for the full minute, to when assistance from the system is turned on ($\kappa > 1.0$), where the completion rate increased to 60% and 80% for $\kappa = 2.0$ and 3.0, respectively. There is, however, not a significant difference in successes between the two assistance levels, $\kappa = 2.0$ and 3.0. The high variation in the results from the normalized successes with an assistance factor of 1.0 is explained by the fact that some individuals were strong enough to complete the whole trial without stopping and their scores were roughly comparable to their trials with assistance. From this, it can be concluded that assistance is helpful up to the point that it allows a person to complete a task, but does not produce a significant difference after that point.

Next, the results from both the tasks with and without moment compensation for the peg-in-hole task with the reacher bar were plotted. As with the peg-in-hole task, the results were normalized for each user over each scaling factor, but here they were also normalized across the maximum number of completions across the tasks with and without moment compensation

$$N_i' = \frac{N_i}{\max\left(N_{i,participant},\ N_{i,participant,mcomp}\right)} \tag{21}$$

This was done so that meaningful comparisons between these two sub-tasks could be made. The normalized number of successes with the bar attached as well as the fraction of users that were able to complete the task for the whole minute are plotted in Figure 11. The data collected during the experiments was tabulated and can be found in Table 6 and the participant normalized data that is plotted can be found in Table 7.

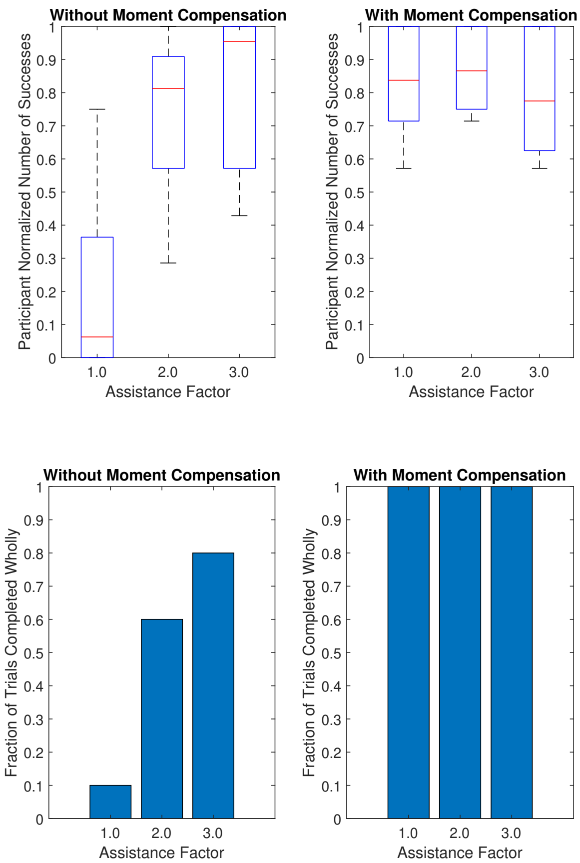

Fig. 11. Participant normalized number of successes and task completion rate at each scaling factor for the peg-in-hole tasks with the reacher bar.

It can be seen that for the trials without moment compensation at a scaling factor of 1.0 (no assistance), there was a sharp increase in the number of individuals that were unable to complete the tasks for the full minute. Similarly, there was a sharp increase in the number of successes for high assistance factors as well. In contrast, it can be seen that all users were able to complete the task for the full minute with the moment compensation turned on. This is indicative of the users' difficulty with supporting a large amount of torque while manipulating objects with a reacher. Looking further into the results with moment compensation on, it can be seen that there was no significant difference between the different levels of compensation from the mass. From this, it can be concluded that reducing the moments is very important for users to be able to complete tasks at a distance using a reacher bar. This type of assistance would therefore likely prove useful for activities of daily living such as placing a book on a shelf or grabbing a play toy from far across the room.

Comparing the number of successes between the tasks with and without moment compensation, it can be seen that the median for the number of successes is slightly higher for the trial with maximum assistance but no moment compensation than any of the trials with moment compensation turned on. This can be explained due to the fact that although the moment compensation assisted users in completing the task, it removed some of the haptic feedback that they got from the environment, thereby making the task slightly more difficult to perform.

The results from the questionnaire after this trial can be found in Table 8 and the averaged data can be found in Figure 12. From the responses, it can be seen that users overall rated the system quite well and that they found the lifting assistance system to be quite useful.

Overall, it can be seen that the force scaling system was beneficial in assisting participants in completing the peg in hole insertion tasks. A strong trend can be seen, for trials without moment compensation, where increasing assistance level significantly increased the percentage of participants who could complete the tasks. Though all the participants were able to complete the task with the moment compensation turned on at every scaling factor, the lack of torque haptic feedback from the environment likely made the task slightly more difficult to perform.

5.3. *Usability and Overall Results*

From the results presented above, it may be concluded that the system presented in this paper is able to scale a user's forces and torques that are applied to the environment, while still retaining their sense of the weight of the objects that they are interacting with. The participants that were involved in this study all rated the system very well in terms of usability and usefulness.

Table 6. Number of participant successes at each assistance factor for the peg-in-hole tasks with the reacher bar.

Participant Number	Assistance Factor					
	Without Moment Compensation			With Moment Compensation		
	1.0	2.0	3.0	1.0	2.0	3.0
1	0*	3*	7	4	5	4
2	0*	5*	5	4	5	4
3	1*	6	8	6	7	6
4	0*	5	4	5	7	4
5	4*	7	8	7	6	6
6	0*	4*	4*	7	7	7
7	0*	6	6	6	5	5
8	6	7	7	8	6	5
9	4*	10	10	10	10	11
10	1*	2*	3*	5	6	7

* indicates that the participant did not complete the trial fully.

Table 7. Participant normalized number of successes at each assistance factor for the peg-in-hole tasks with the reacher bar.

Participant Number	Assistance Factor					
	Without Moment Compensation			With Moment Compensation		
	1.0	2.0	3.0	1.0	2.0	3.0
1	0.00*	0.43*	1.00	0.57	0.71	0.57
2	0.00*	1.00*	1.00	0.80	1.00	0.80
3	0.13*	0.75	1.00	0.75	0.88	0.75
4	0.00*	0.71	0.57	0.71	1.00	0.57
5	0.50*	0.88	1.00	0.88	0.75	0.75
6	0.00*	0.57*	0.57*	1.00	1.00	1.00
7	0.00*	1.00	1.00	1.00	0.83	0.83
8	0.75	0.88	0.88	1.00	0.75	0.63
9	0.36*	0.91	0.91	0.91	0.91	1.00
10	0.14*	0.29*	0.43*	0.71	0.86	1.00

* indicates that the participant did not complete the trial fully.

Table 8. Tabulated answers to the usability questionnaire for both peg-in-hole tasks.

	Number of Participants					
Rating Given for Question	0	1	2	3	4	5
Manipulability					1	9
Confidence in System				1	2	7
Position Accuracy					2	8
Usefulness of Lifting Assistance					2	8

The effect of task learning was likely mostly mitigated through the randomization of the task order, the order of system assistance factors within the tasks, and differing the user groups between the task tests. Arm lengths and participant pose were not considered during this study though they may have an effect on the performance of each individual. However, the normalization of the presented experimental results with respect to each participant should reduce the impact of these effects. Lastly, although recruiting able-bodied participants to evaluate a system designed for people with physical impairments is not ideal, it allows for an initial insight into the potential assistive uses for a force scaling admittance controlled system for people with a physical disability. This is especially true considering that the peg-in-hole tasks were designed so that many participants were unable to complete them without assistance. This parallels very well with individuals who are with conditions such as Duchenne muscular dystrophy or cerebral palsy and may find themselves unable to complete some activities of daily living without assistance.

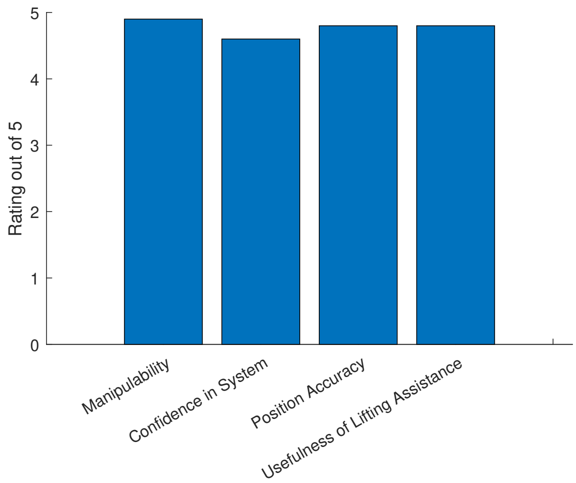

Fig. 12. Answers to the usability questionnaire for both peg-in-hole tasks.

6. Conclusions

In this paper, an admittance controlled 6 degree-of-freedom assistive robotic system was presented. This system was implemented with the goal of improving the ability of a child with disabilities to manipulate heavy objects in space, which is vital for play activities, while still maintaining their sense of what they are lifting. The system used two force-torque sensors, an assistance factor to amplify the force that the user can apply, and an admittance controller to allow for easy movement of the robotic system. Two user-studies were done to evaluate the usability of the system. First, ten able-bodied individuals were asked to order a series of buckets with identical appearances and weights of 1.5 kg, 2.0 kg, 2.5 kg, and 3.0 kg from lightest to heaviest at different assistance factors of the system. It was shown that the force amplification ability of the system did not significantly detract from a user's ability to discriminate masses. Second, ten able-bodied individuals were asked to perform peg-in-hole insertion tasks to evaluate the user positional precision and usefulness of the force amplification ability of the system both with and without a reacher bar. It was shown that the system had a positive effect on the ability of the user to perform a peg-in-hole insertion task when the assistance was needed for them to be able to perform the task for the whole minute. Increasing amounts of assistance did not provide significant effect once participants were able to perform the task for the whole minute. For the case with the modular reacher bar attached, it was shown that moment compensation had a very positive effect in assisting users in completing the task. Future works will involve performing user trials with individuals (mostly children) with upper-body weakness and RoM issues − the target population of this system. Additionally, different end effectors and tasks may be considered to further evaluate the efficacy of the system, across a broad spectrum of activities of daily living. In the presented system, the scaling factor α is applied equally in all DoFs; however, in the future different scaling factors could be implemented for each DoF should the user require more assistance with certain motions. These assistance factors may be further optimized to better assist users, on a per-user basis, when the modular reacher bar is attached.

Acknowledgments

This research was supported by the Canada Foundation for Innovation (CFI), the Government of Alberta, the Natural Sciences and Engineering Research Council (NSERC) of Canada, the Canadian Institutes of Health Research (CIHR), and the Alberta Economic Development, Trade and Tourism Ministry's Grant to Centre for Autonomous Systems in Strengthening Future Communities.

References

[1] Office of the United Nations High Commissioner for Human Rights, Convention on the Rights of the Child (1989).

[2] C. S. Tamis-LeMonda, J. D. Shannon, N. J. Cabrera and M. E. Lamb, Fathers and Mothers at Play With Their 2- and 3-Year-Olds: Contributions to Language and Cognitive Development, *Child Development* **75** (dec 2004) 1806–1820.

[3] J. L. Frost, Neuroscience, Play, and Child Development., *IPA/USA Triennial National Conference (Longmont, CO, June 18-21, 1998).*, (IPA/USA, jun 1998).

[4] K. R. Ginsburg, American Academy of Pediatrics Committee on Communications and American Academy of Pediatrics Committee on Psychosocial Aspects of Child and Family Health, The importance of play in promoting healthy child development and maintaining strong parent-child bonds., *Pediatrics* **119** (jan 2007) 182–91.

[5] T. Klein, G. J. Gelderblom, L. de Witte and S. Vanstipelen, Evaluation of short term effects of the IROMEC robotic toy for children with developmental disabilities, *2011 IEEE International Conference on Rehabilitation Robotics*, **2011**, (IEEE, jun 2011), pp. 1–5.

[6] I. Sakamaki, K. Adams, M. F. G. Medina, J. L. C. Cruz, N. Jafari, M. Tavakoli and H. Janz, Preliminary testing by adults of a haptics-assisted robot platform designed for children with physical impairments to access play, *Assistive Technology* **30** (oct 2018) 242–250.

[7] N. Jafari, K. D. Adams, M. Tavakoli and S. Wiebe, Development of an Assistive Robotic System with Virtual Assistance to Enhance Play for Children with Disabilities: A Preliminary Study, *Journal of Medical and Biological Engineering* **38** (feb 2018) 33–45.

[8] N. Jafari, K. Adams, M. Tavakoli, S. Wiebe and H. Janz, Usability testing of a developed assistive robotic system with virtual assistance for individuals with cerebral palsy: a case study, *Disability and Rehabilitation: Assistive Technology* **13** (aug 2018) 517–522.

[9] N. Jafari, K. D. Adams and M. Tavakoli, Haptics to improve task performance in people with disabilities: A review of previous studies and a guide to future research with children with disabilities, *Journal of Rehabilitation and Assistive Technologies Engineering* **3** (jun 2016).

[10] M. Oostermeijer, A. J. H. Boonen and J. Jolles, The relation between children's constructive play activities, spatial ability, and mathematical word problem-solving performance: a mediation analysis in sixth-grade students., *Frontiers in psychology* **5** (2014) p. 782.

[11] D. A. Christakis, F. J. Zimmerman and M. M. Garrison, Effect of Block Play on Language Acquisition and Attention in Toddlers, *Archives of Pediatrics & Adolescent Medicine* **161** (oct 2007) p. 967.

[12] A. Q. Keemink, H. van der Kooij and A. H. Stienen, Admittance control for physical human–robot interaction, *The International Journal of Robotics Research* **37** (sep 2018) 1421–1444.

[13] N. Hogan, Impedance Control: An Approach to Manipulation: Part I—Theory, *Journal of Dynamic Systems, Measurement, and Control* **107** (mar 1985) 1–7.

[14] E. J. Gibson, Exploratory behavior in the development of perceiving, acting, and the acquiring of knowledge., *Annual review of psychology, Vol. 39.*, *Annual review of psychology.* (Annual Reviews, Palo Alto, CA, US, 1988), pp. 1–41.

[15] M. Corrigan and R. Foulds, Admittance Control of the Intelligent Assistive Robotic Manipulator for Individuals with Duchenne Muscular Dystrophy: A Proof-of-Concept Design, *Journal of Rehabilitation Robotics* **3** (may 2015) 1–5.

[16] I.-Y. Jung, J. H. Chae, S. K. Park, J. H. Kim, J. Y. Kim, S. J. Kim and M. S. Bang, The Correlation Analysis of Functional Factors and Age with Duchenne Muscular Dystrophy, *Ann Rehabil Med* **36** (feb 2012) 22–32.

[17] M. Oskoui, F. Coutinho, J. Dykeman, N. Jetté and T. Pringsheim, An update on the prevalence of cerebral palsy: a systematic review and meta-analysis, *Developmental Medicine & Child Neurology* **55** (jun 2013) 509–519.

[18] M. de Bruin, M. J. C. Smeulders and M. Kreulen, Why is joint range of motion limited in patients with cerebral palsy?, *Journal of Hand Surgery (European Volume)* **38** (apr 2012) 8–13.

[19] I. Sakamaki, C. E. P. del Campo, S. A. Wiebe, M. Tavakoli and K. Adams, Assistive technology design and preliminary testing of a robot platform based on movement intention using low-cost brain computer interface, *2017 IEEE International Conference on Systems, Man, and Cybernetics (SMC)*, (2017), pp. 2243–2248.

[20] C. Rossa, M. Najafi, M. Tavakoli and K. Adams, Nonlinear workspace mapping for telerobotic assistance of upper limb in patients with severe movement disorders, *2017 IEEE International Conference on Systems, Man, and Cybernetics (SMC)*, (2017), pp. 2255–2260.

[21] F. Gosselin, F. Ferlay and A. Janot, Development of a New Backdrivable Actuator for Haptic Interfaces and Collaborative Robots, *Actuators MDPI* **5** (jun 2016).

[22] N. Hogan and S. P. Buerger, 19 impedance and interaction control (2004).

[23] R. J. Adams and B. Hannaford, Stable haptic interaction with virtual environments, *IEEE Transactions on Robotics and Automation* **15**(3) (1999) 465–474.

[24] W. S. Newman and Y. Zhang, Stable interaction control and coulomb friction compensation using natural admittance control, *Journal of Robotic Systems* **11** (jan 1994) 3–11.

[25] J. Carriere, J. Fong, T. Meyer, R. Sloboda, S. Husain, N. Usmani and M. Tavakoli, *An Admittance-Controlled Robotic Assistant for Semi-Autonomous Breast Ultrasound Scanning* apr 2019.

[26] J. Fong and M. Tavakoli, Kinesthetic teaching of a therapist's behavior to a rehabilitation robot, *2018 International Symposium on Medical Robotics (ISMR)*, (March 2018), pp. 1–6.

[27] J. Fong, R. Ocampo, D. P. Gross and M. Tavakoli, A Robot with an Augmented-Reality Display for Functional Capacity Evaluation and Rehabilitation of Injured Workers, *2019 IEEE 16th International Conference on Rehabilitation Robotics (ICORR)*, (2019), pp. 181–186.

[28] F. Dimeas and N. Aspragathos, Online stability in human-robot cooperation with admittance control, *IEEE Transactions on Haptics* **9** (April 2016) 267–278.

[29] R. Rajan, H. A. and R. James, State Space Representation of Fractional-Order Low-Pass Filters, *2015 Fifth International Conference on Advances in Computing and Communications (ICACC)*, (IEEE, sep 2015), pp. 155–158.

[30] M. C. Yip, M. Tavakoli and R. D. Howe, Performance analysis of a manipulation task in time-delayed teleoperation, *2010 IEEE/RSJ International Conference on Intelligent Robots and Systems*, (2010), pp. 5270–5275.

[31] B. Hannaford, L. Wood, D. A. McAffee and H. Zak, Performance evaluation of a six-axis generalized force-reflecting teleoperator, *IEEE Transactions on Systems, Man, and Cybernetics* **21**(3) (1991) 620–633.

Jakub Piwowarczyk completed his B.Sc. in Mechanical Engineering with the Biomedical Option at the University of Alberta, Canada in 2019. He is currently a Research Assistant in the Department of Computing Science at the University of Alberta. His research interests include medical robotics, assistive robotics, and mechatronics.

Jay Carriere earned his B.Sc. in Electrical Engineering and Ph.D. in Biomedical Engineering from the University of Alberta, Alberta, Canada in 2011 and 2019, respectively. He is currently a Post-Doctoral Research Fellow in the Department of Electrical and Computer Engineering at the University of Alberta. His research interests involve medical robotics, medical image processing, image-guided robotic-assisted surgery, and collaborative robotics.

Kim Adams is an Associate Professor with the Faculty of Rehabilitation Medicine at the University of Alberta, Edmonton, AB, Canada, and a Research Affiliate with the Glenrose Rehabilitation Hospital. She received her BSc and MSc in Engineering, and her PhD degree in Rehabilitation Science from the University of Alberta, Canada, in 2011. Dr. Adams's research interests are assistive technology design, development and evaluation, including alternative access methods and assistive robots for children with physical disabilities to engage in play and learning activities.

Mahdi Tavakoli is a Professor in the Department of Electrical and Computer Engineering, University of Alberta, Canada. He received his BSc and MSc degrees in Electrical Engineering from Ferdowsi University and K.N. Toosi University, Iran, in 1996 and 1999, respectively. He received his PhD degree in Electrical and Computer Engineering from the University of Western Ontario, Canada, in 2005. In 2006, he was a post-doctoral researcher at Canadian Surgical Technologies and Advanced Robotics (CSTAR), Canada. In 2007-2008, he was an NSERC Post-Doctoral Fellow at Harvard University, USA. Dr. Tavakoli's research interests broadly involve the areas of robotics and systems control. Specifically, his research focuses on haptics and teleoperation control, medical robotics, and image-guided surgery. Dr. Tavakoli is the lead author of Haptics for Teleoperated Surgical Robotic Systems (World Scientific, 2008). He is a Senior Member of IEEE and an Associate Editor for IEEE/ASME Transactions on Mechatronics, Journal of Medical Robotics Research, Control Engineering Practice, and Mechatronics.